RESEARCH ARTICLE
PLANETARY SCIENCES

Earth and Planetary Physics
10: 374–384, 2026
doi: 10.26464/epp2026035

The activity characteristics and mechanisms of long-period comets

YingQi Wu[1,2], JianChun Shi[1*], Man-To Hui[1], and Xian Shi[1]

[1]Shanghai Astronomical Observatory, Chinese Academy of Sciences, Shanghai 200030, China;

[2]School of Astronomy and Space Sciences, University of Chinese Academy of Sciences, Beijing 101408, China

Key Points:

- Long-period comets and short-period comets exhibit significant differences in activity.
- The activity of long-period comets may be facilitated by a variety of mechanisms.
- Long-period comets exhibit large variations in color, and display diverse tail morphologies.

Citation: Wu, Y. Q., Shi, J. C., Hui, M.-T., and Shi, X. (2026). The activity characteristics and mechanisms of long-period comets. *Earth Planet. Phys.*, *10*(2), 374–384. http://doi.org/10.26464/epp2026035

Abstract: Comets are small celestial bodies orbiting around the Sun. They are remnants left over from the formation of the solar system; their interiors store original material of the planetary disk within the solar system. They are thus "fossils" for studying the early solar system. According to their orbital periods, comets are classified as long-period comets (orbital period $P > 200$ years) and short-period comets ($P < 200$ years). Long-period comets originate from the Oort Cloud. Compared to short-period comets, they enter the inner solar system less frequently and contain more primitive materials. Studying long-period comets helps us understand the origin of the solar system and reveals characteristics of the Oort Cloud. This paper begins with a summary of our extensive survey of the literature regarding methods of observing comets and foci of comet studies. We introduce systematically the main parameters currently used to assess the activity of long-period comets, including gas production rate, dust production rate, dust properties, morphological characteristics, etc. Subsequently, we discuss in depth the activity mechanisms of long-period comets, covering not only the water ice sublimation-driven mechanism (similar to that of short-period comets) but also various mechanisms that may dominate the activity of long-period comets in the low-temperature environment at the aphelion. These mechanisms include the sublimation of CO or CO_2 gas ice, the polymerization reaction of cyanides, the crystallization of amorphous water ice, the annealing process of amorphous water ice, the thermal decomposition effect, and the electrostatic supercharge phenomenon. We then summarize the evolving activity of long-period comets as they travel from the Oort Cloud to the vicinity of their perihelions. We analyze unique properties of long-period comets, including such special phenomena as changes in dust color, coma structure, and tail structure. Finally, we summarize currently unresolved scientific questions, and then the entire paper.

Keywords: comets; long-period comets; activity

1. Introduction

Comets are generally regarded as vestiges from the formation of our solar system, approximately 4.6 billion years ago, that retain pristine material information. Comets may have collided with Earth during the evolutionary process of the solar system, delivering water and organic substances to our planet (Hartogh et al., 2011). The comet nucleus is often described as a "dirty snowball", mainly composed of ice and dust (Geheimenrath and Bessel, 1836). Comet ices consist primarily of water, carbon monoxide, carbon dioxide, methane, ammonia, and other volatile species (Whipple, 1950; Bockelée-Morvan and Biver, 2017). When the ices in the cometary nucleus sublimate due to solar heating, a coma forms, appearing as a diffuse layer composed of gas and dust around the nucleus. In the coma, apart from water, carbon monoxide and carbon dioxide are typically the most abundant components (Mumma and Charnley, 2011).

Comets are often classified into long-period and short-period populations based on an orbital-period threshold of 200 years. In general, long-period comets are thought to originate from the Oort Cloud, while short-period comets are commonly associated with the Kuiper Belt (Oort, 1950; Kuiper, 1951). Compared with short-period comets, long-period comets typically exhibit higher absolute magnitudes and stronger activity (Betzler et al., 2023). This difference arises because, in the Oort Cloud, long-period comets remain in an extremely cold environment with almost no sublimation, thereby staying in a “dormant” state. Under such conditions, their interior ices and dust remain stably frozen; only when perturbed by passing stars or Galactic tides can their orbits be deflected into the inner solar system. Many long-period comets entering the inner solar system are thought to retain abundant primitive volatiles and dust components, making them valuable probes of early solar system evolution and the environ-

First author: Y. Q. Wu, yqiwu@shao.ac.cn
Correspondence to: J. C. Shi, jcshi@shao.ac.cn
Received 10 SEP 2025; Accepted 23 JAN 2026.
First Published online 13 FEB 2026.

ment of the Oort Cloud. Mid-IR photometric observations of comets conducted prior to the era of high-resolution spectroscopy had already revealed the presence of Mg-rich silicate grains (Gehrz et al., 1995); such signatures were detected as early as C/1975 V1 (West). The exceptional brightness of C/1995 O1 (Hale–Bopp), combined with the availability of advanced mid-infrared spectroscopy, enabled a detailed characterization of these materials, including identification of Mg-rich crystalline olivine in its dust coma (Crovisier et al., 1997). The spectral properties of this crystalline component closely resemble those observed in circumstellar dust around young, Vega-type stars, reinforcing the compositional link between long-period cometary dust and dust in protoplanetary environments. Together, these results underline the relevance of long-period comets as key laboratories for investigating the formation conditions and early evolution of the solar system.

This review focuses on the observable properties of long-period comets and how their activity evolves as they approach the Sun. We summarize previous studies on how cometary activity varies with heliocentric distance, on the main mechanisms driving such activity, and on associated changes in coma color and tail morphology. By reviewing observational results from different heliocentric regions, this work aims to provide an overview of typical behaviors of long-period comets and to highlight the importance of comet studies to our understanding of the early evolution of our solar system.

2. Observational Characteristics and Research Methods

Before delving into the characteristics of long-period comets, it is necessary to provide an overview of relevant observational techniques. Comet observations have been made from Earth and spacecraft primarily via optical and infrared imaging, photometry, spectroscopy, radio observations, and polarimetry.

Optical telescopes have commonly employed broadband filters, including those in the Johnson–Cousins system (e.g., B, R, V, I), as well as other photometric systems, to obtain imaging data. The data are then processed through noise reduction and image enhancement techniques; magnitudes of the comet are estimated using photometry with varying aperture sizes. Based on these results, standard magnitudes are obtained after calibration, from which light curves can be constructed and the comet's color index as well as *Afρ* can be calculated. In addition, when coupled with spectrographs, data from optical telescopes can provide cometary spectra. Using classical spectral extraction methods (Horne, 1986), the data can be reduced nearly in real time by removing telluric absorption lines and subtracting the solar continuum contribution. Specific emission or absorption features at given wavelengths can then be identified, allowing inferences about the chemical species present in the comet and their relative abundances.

Radio observations provide an important complement to optical measurements by probing both molecular line emission and continuum emission from large dust grains. Radio spectroscopy enables the detection of key molecular species such as HCN, HCO^+, OH, and NH_3. Unlike optical techniques, which primarily probe daughter species produced by photodissociation, radio spectroscopy traces rotational transitions that are only weakly dependent on solar illumination, although molecular excitation can still involve solar infrared pumping or collisional processes. In addition, radio continuum measurements are sensitive to thermal emission from millimeter- to centimeter-sized dust particles, providing constraints on our ability to determine the abundance and physical properties of large grains in cometary comae. Radio observations therefore are most useful in enabling study of more pristine volatiles originating from deeper layers of the nucleus; they provide access to key dynamical diagnostics, including gas expansion velocities and velocity-resolved line profiles. In addition, radio measurements remain effective even when comets are optically faint or located at small solar elongation angles, making them essential for monitoring temporal variations in gas activity and for characterizing the volatile composition of distant or low-activity comets (Crovisier et al., 2016). Infrared observations offer complementary diagnostics of cometary dust and ice. Near-infrared spectroscopy is sensitive to vibrational bands of volatile ices, such as H_2O, CO, and CO_2, while mid-infrared observations probe the thermal emission of dust and reveal spectral features of silicate minerals, including amorphous and crystalline Mg-rich silicates.

Moreover, polarimetric observations can further yield information on the scattering directions of cometary dust grains induced by electromagnetic interactions, thereby revealing the microscopic physical properties of the dust particles (Bohren and Huffman, 1998; Mishchenko et al., 2010). For example, observations of comets C/2018 V1 (Machholz–Fujikawa–Iwamoto) and C/2023 P1 (Nishimura) reported extremely low degrees of positive linear polarization (Zubko et al., 2020a; Zheltobryukhov et al., 2023). These measurements suggest that the dust of those comets is dominated by Mg-rich silicate particles. Such results demonstrate the capability of polarimetric observations to probe the physical properties and composition of cometary dust, complementing optical and radio observations.

In addition to ground-based optical and spectroscopic observations, space-based platforms offer unique advantages for cometary studies. Space-based infrared observations are not affected by telluric CO_2 absorption and therefore enable direct detection of CO and CO_2 in comets, with notable examples provided by NEOWISE (Milewski et al., 2024). Regarding in situ comet exploration, the ESA Rosetta mission provided unprecedented constraints on gas and dust emission processes through continuous monitoring of the nucleus and coma of comet 67P/Churyumov–Gerasimenko. Although 67P is a Jupiter-family comet, the mission established a physical framework for interpreting cometary activity, including the spatial and temporal decoupling between gas and dust emissions, heterogeneous surface activity, and the role of different volatile species in driving mass loss (Taylor et al., 2017 and references therein). These results have informed modern analyses of gas and dust production rates in comets, which commonly employ refined Haser-type models for gas species and Monte Carlo dust tail simulations to constrain dust size distributions, ejection velocities, and mass-loss rates. While direct in situ measurements are currently unavailable for long-period comets, such modeling approaches—originally calibrated and validated using missions such as Rosetta—provide a

valuable basis for interpreting remote observations of LPC activity.

Studies of cometary activity typically involve measurements of multiple parameters, including gas production rates, dust production rates, dust properties, and morphological features. Gas production rates are generally derived from observations of spectral line fluxes, which are converted into production rates using the Haser model of cometary coma dynamics (Haser, 1957) or other coma models. Dust production is commonly characterized by *Afρ*, a parameter that provides a proxy for the dust mass loss rate under the assumption of steady-state, approximately isotropic outflow and a $1/\rho$ surface brightness profile, and is therefore often used as an indicator of cometary dust activity (A'Hearn et al., 1984). Dust properties, such as particle size distributions, can be inferred from observations of scattered sunlight, including broadband photometry, polarimetry, and scattering spectra from the optical to near-infrared. Optical scattering models, based on Mie theory for homogeneous spheres or the discrete dipole approximation (DDA) for irregular grains, are commonly used to interpret these observations. Other approaches include agglomerated debris particle models and core–mantle or porous grain models (e.g., Kolokolova et al., 2004; Lasue et al., 2009; Zubko et al., 2011, 2014). These models adopt optical constants from laboratory measurements or the literature to constrain dust size distributions. In this review, we limit the discussion to scattering-based diagnostics; thermal emission measurements in the infrared and sub-millimeter are not considered here. Broadband photometry records continuum intensities across different bands. The color index, defined as the difference between magnitudes measured in two bands (e.g., B–V, V–R), characterizes the continuum slope. By comparing the comet's color index with that of the Sun, color variations can be identified, providing further insights into cometary activity. Monte Carlo models are often used to simulate the dynamical evolution of dust particles with various size and velocity distributions under solar radiation pressure and gravity (Fulle, 1989). These simulations generate synthetic coma or dust tail morphologies that can be compared with observations to constrain dust size and velocity distributions and other physical properties (Moreno et al., 2012, 2014; Moreno, 2022). In morphological studies, such models can also describe the coupled dynamical and optical processes of dust and gas, offering key support for interpreting tail structures, dust velocity fields, and particle properties. A widely applied technique in morphological analysis is the Larson–Sekanina image enhancement method, which performs radial and angular differencing on images to highlight hidden structural features (Larson and Sekanina, 1984). The validity of these enhanced features is further tested by applying azimuthal averaging to distinguish genuine structures from artifacts, ensuring that the morphological details revealed are real.

3. Activity-Driving Mechanisms of LPCs

As noted in the introduction, comets are composed of a mixture of ices and dust, and thus their activity is primarily driven by the sublimation of water ice and volatile ices. In the present Solar System, different volatiles become thermally active over distinct but overlapping ranges of heliocentric distances. Water ice (H_2O) sublimation dominates cometary activity primarily in the inner Solar System, typically within a few astronomical units, whereas more volatile species such as CO_2 and CO are capable of driving activity at substantially larger distances. Heliocentric distance, often associated with the so-called "snow lines" (approximately a few au for H_2O, several to ~10 au for CO_2, and tens of au for CO), is commonly used as an order-of-magnitude indicator, rather than precise physical boundaries (e.g., Qi CH et al., 2013; Musiolik et al., 2016). In practice, the onset of sublimation for a given volatile is expected to vary depending on conditions near the nucleus surface, including volatile abundance, nucleus size, thermal inertia, porosity, and albedo. Long-period comets are characterized by large semimajor axes, whereas short-period comets are confined to much smaller orbits. Owing to their frequent perihelion passages and prolonged thermal evolution, short-period comets are expected to experience significantly greater depletion of highly volatile ices in their near-surface layers, compared to long-period comets that may still be driven by the sublimation of supervolatile ices at large heliocentric distances. The onset of this process depends on the latent heat of sublimation and the equilibrium surface temperature of the nucleus, which in turn is controlled by parameters such as heliocentric distance, albedo, surface emissivity, rotation rate, pole orientation, and thermal diffusivity—all of which affect subsurface heat transport. Evidently, cometary activity at heliocentric distances $r \lesssim 2$–3 au is driven mainly by the sublimation of water ice. In fact, solutions to the surface energy balance equation indicate that even at $r = 5.2$ au, the gas flux from sublimating water ice is sufficient to lift small particles (< 0.1 μm) from the surface (Meech and Svoreň, 2004; Prialnik et al., 2004).

Beyond 5.2 au, additional mechanisms must be invoked to account for cometary activity. Several possible processes have been proposed to drive the activity of long-period comets, including: the sublimation of CO or CO_2 ices (Houpis and Mendis, 1981; Luu, 1993), polymerization of hydrogen cyanide (Rettig et al., 1992), crystallization of amorphous water ice (Prialnik, 1992; Gronkowski and Smela, 1998), annealing of amorphous water ice (Meech et al., 2009), thermal fracture, and electrostatic supercharging effects (Jewitt et al., 2019).

Observations of distant long-period comets provide growing—but still incomplete—evidence that supervolatile ices play a key role in sustaining activity at heliocentric distances $r \gtrsim 5$ au. For example, CO has been directly detected in a few comets at large distances, such as C/2017 K2 (PanSTARRS) beyond 6 au (Meech et al., 2017; Yang B et al., 2021), while high-resolution spectroscopy indicates that CO_2 can also play a significant, or even dominant, role at smaller distances (~2.8 au) (Cambianica et al., 2023). Polarimetric observations at ~6–7 au suggest further that the coma at that distance is largely dominated by dust rather than gas (Zhang QC et al., 2022; Kochergin et al., 2023). However, the available observational evidence is not uniform across different objects and heliocentric distances. Some comets, such as C/1980 E1 (Bowell; formerly 1980b), show no detectable CO emission. At heliocentric distances near ~3.3 au, the non-detection of gas emissions may also arise from observational limitations, as large parent-molecule scale lengths can significantly reduce surface brightness; conse-

quently, the contribution of CO_2 to the observed activity remains uncertain in such cases (Houpis and Mendis, 1981; Schulz et al., 1998).

Despite these limitations on individual detections, statistical studies provide complementary support for supervolatile-driven activity at large heliocentric distances. A'Hearn et al. (2012) found that beyond 5 au, the production rates of CO or CO_2 increase as heliocentric distance decreases, suggesting that cometary activity at $r > 5$ au is primarily driven by supervolatile ices. Measurements of CO and CO_2 in 25 comets further show that CO_2 outgassing generally correlates more strongly with water production than CO does (Harrington Pinto et al., 2022). In addition, several models suggest that even Oort Cloud comets are significantly processed by cosmic ray irradiation, which depletes CO in the outermost ~10 m of their nuclei, while CO_2 and CH_4 remain largely unaffected (Gronoff et al., 2020; Maggiolo et al., 2020). Together, these findings suggest that, for comets making their first passage into the inner Solar System (often referred to as "dynamically new" comets), activity prior to entering the water–ice snow line is driven primarily by the sublimation of CO and CO_2 ices.

HCN is a common interstellar molecule; its polymers may form on the surfaces of icy grains irradiated by ultraviolet photons or energetic ions. These grains subsequently aggregate and constitute cometary bodies. Thus, HCN polymers may be incorporated into different regions of a comet's interior. Because HCN is less volatile than water, it may undergo further chemical evolution as the comet enters its active phase, gradually accumulating near the surface and eventually forming an inert crust. In amorphous water ice, two HCN molecules are in nearest-neighbor contact about 24% of the time, so the probability of their polymerization increases significantly with rising temperature. The formation of HCN polymers may also result from ongoing chemical evolution within the nucleus. Under solar UV irradiation, HCN molecules absorb photons and enter electronically excited states, in which their electronic structure exhibits pronounced radical character, primarily localized on the carbon atom. These excited radicals readily combine with another HCN molecule to form HCN dimers (Rettig et al., 1992). The polymerization of HCN is an exothermic process, which can readily trigger cometary outbursts and may also induce the crystallization of amorphous water ice.

During the crystallization of amorphous water ice, substantial outgassing occurs, which in turn governs the local temperature distribution. Water vapor released in this process recondenses and liberates latent heat, preventing the newly crystallized layers from cooling. Consequently, even at large heliocentric distances, as long as crystallization continues, subsurface layers of the nucleus—tens to hundreds of meters deep—can reach relatively high temperatures (~170 K). The released gases migrate both inward and outward; the latter can escape from the nucleus surface (Prialnik, 1992; Prialnik and Jewitt, 2024). The crystallization of amorphous water ice generates most of the energy responsible for cometary outbursts; part of this energy drives the release of trapped volatiles (e.g., CO or CO_2), leading to a sudden acceleration in their sublimation rates. At the same time, it produces severe stress that erodes and fragments the cometary surface (Gronkowski and Smela, 1998). Similarly, annealing of amorphous ice—when heated to below the amorphous-to-crystalline transition temperature ($T \sim 137$ K)—can release significant amounts of trapped gases and expel large dust particles at low velocities. This process is considered a key driver of cometary activity when a comet first enters the inner solar system (Meech et al., 2009).

However, Jewitt et al. (2019), in explaining the activity of C/2017 K2 (PanSTARRS) under distant and low-temperature conditions, argued that CO sublimation alone is insufficient to expel larger dust particles, while the aforementioned mechanisms are also ineffective at such low temperatures. They therefore proposed two additional possibilities: (1) thermal fracture, and (2) electrostatic supercharging. These mechanisms may assist in releasing larger particles from the cometary surface under distant, low-temperature environments.

4. Evolution of Long-Period Cometary Activity from Aphelion to Perihelion

Several long-period comets have been observed to exhibit clear activity at large heliocentric distances, well beyond the water–ice sublimation zone. For example, C/2017 K2 (PANSTARRS) and C/2010 U3 (Boattini) were already active at heliocentric distances exceeding 20 au; activity at such distances has also been reported for other long-period comets. These observations demonstrate that cometary activity can occur at very large heliocentric distances; such distant activity has been commonly interpreted as being driven by the sublimation of supervolatile ices (e.g., CO and CO_2), possibly supplemented by other processes such as phase transitions in amorphous ice (Hui M-T et al., 2017; Jewitt et al., 2017; Meech et al., 2017; and references therein).

Long-period comets (LPCs) exhibit significant changes in activity as they travel from the distant Oort Cloud to perihelion. At heliocentric distances beyond 10 au, short-period comets generally show only weak activity; in contrast, some long-period comets can exhibit substantial activity even beyond 10 au, primarily driven by the sublimation of supervolatile ices such as CO and CO_2. For example, C/2017 K2 (PANSTARRS) was already active at a heliocentric distance of 23.7 au in 2013, but was discovered only by the Pan-STARRS1 (PS1) survey on May 21, 2017, at 16.09 au (Jewitt et al., 2017; Meech et al., 2017). After a comet reaches a heliocentric distance of 5.2 au, the gas flux from sublimating water ice is already sufficient to lift small particles (<0.1 μm) from the surface, resulting in a certain level of activity. Once a long-period comet crosses the water–ice snow line at ~3 au, sublimation of water ice intensifies. Combined with the ongoing sublimation of other volatile ices, water ice sublimation effectively releases additional volatiles, ice grains, and dust from the nucleus, resulting in a sharp increase in dust and gas production rates and a pronounced enhancement of cometary activity (Weaver, 1989; Meech and Svoreň, 2004; Prialnik et al., 2004).

Near perihelion, cometary activity becomes significantly more intense, with multiple outbursts occurring over short timescales, and in some cases leading to nucleus disruption. For instance, high-cadence monitoring of comet C/2021 A1 (Leonard) revealed at least six distinct outbursts characterized by concurrent enhancements in gas emissions and *Afρ* measurements (Lippi et al., 2023), while a later outburst at a heliocentric distance of

approximately 0.7 au marked the onset of its disintegration (Garcia et al., 2024). A notable example of nucleus fragmentation is comet C/2019 Y4 (ATLAS), which underwent a progressive disintegration during the approximately 70 days preceding perihelion, at heliocentric distances between 1.8 and 0.6 au. Although no discrete outbursts prior to its disintegration have been reported, the comet exhibited pronounced brightness variations accompanied by a gradual loss of central condensation and emergence of multiple fragments (Hui M-T and Ye QZ, 2020; Ye QZ et al., 2021). Imaging observations documented the morphological evolution of the pseudo-nucleus and the formation of fragment clusters during the breakup process (Sonka et al., 2020; Ye QZ et al., 2021). The observed brightness and color evolution, including a significant bluing of the dust continuum, has been interpreted as due to the exposure and sublimation of fresh subsurface volatiles during the disintegration (Hui M-T and Ye QZ, 2020; Ye QZ et al., 2021). Polarimetric observations obtained before and after the breakup reveal a marked increase in positive polarization, suggesting an enhanced contribution from carbonaceous dust grains in the coma (Zubko et al., 2020b). Complementary spectroscopic and photometric studies further show that, despite the dramatic dust evolution and relatively low dust content, the gas composition remained typical of Oort cloud comets (Ivanova et al., 2021; Zhao RN et al., 2024).

Due to the enhanced gas release driven by water–ice sublimation at these heliocentric distances, some comets exhibit pronounced color variations. Analyses of coma morphology for comets within 3 au show that long-period comets consistently exhibit color changes within apertures of ~20,000 km, consistent with increased gas production driven by water–ice sublimation (Holt et al., 2024). Dynamically new comets, upon entering $r < 3$ au, show a decrease in brightness growth rate from 12.8 mag/log au to 7 mag/log au, whereas returning comets (with prior passages through the inner Solar System) within $r < 6$ au display slower brightness increases (~14 mag/log au) and exhibit more scattering in brightening behavior. Overall, dynamically new comets are intrinsically brighter than returning comets, and the correlations between their brightness parameters are more stable and tighter (Lacerda et al., 2025). Returning comets tend to exhibit color changes closer to the Sun, likely because their volatiles have been depleted during previous perihelion passages, are buried deeper, or their higher dust-to-gas ratios delay observable gas release (Holt et al., 2024).

A subset of comets with extremely Sun-approaching orbits, the Kreutz-group sungrazing comets, are usually discovered only a few days before perihelion. For example, C/2024 S1 (ATLAS) was detected at a perihelion distance of merely 0.008 au, reached peak brightness near 0.075 au, and subsequently faded. During its last observation at 0.02 au from the Sun, its brightness had decreased by a factor of ~20 (Jewitt et al., 2025).

If a long-period comet does not undergo disintegration during its first perihelion passage, it may return in the future. A notable example is C/2017 K2 (PanSTARRS), a returning long-period comet whose previous perihelion passage occurred approximately 3 million years ago. During its current return (evolving from a heliocentric distance of 15.9 au to 13.8 au), it still exhibited significant activity (Jewitt et al., 2019). This example illustrates that some returning long-period comets can maintain strong activity at large heliocentric distances, highlighting the diversity of cometary behavior without implying support for a particular trend in the broader population.

5. The Effect of Long-Period Cometary Activity on Coma Color

The primary volatiles of comets are water (H_2O), carbon monoxide (CO), carbon dioxide (CO_2), and other molecules such as CH_3OH, H_2CO, HCN, and NH_3. Long-period comets tend to be richer in CO and CO_2, although the relative abundances vary among different comets, showing significant diversity. Dust in comets, including various silicates, exhibits different colors, which are generally determined by the physical properties of the dust grains, such as their size distribution and chemical composition, and are largely independent of the number of particles within the observational aperture (Betzler et al., 2017; Luk'yanyk et al., 2019).

Cometary color is typically quantified using the color index (e.g., B–V, V–R); a smaller difference compared to the Sun indicates a bluer color, while a larger difference indicates a redder color. However, gas emissions, particularly in the B and V bands, may contaminate broadband photometry data and thus limit the use of photometry in determining dust color. In addition to color index data, cometary dust color can be quantified using a comet's spectral slope (or reflectance gradient), which measures the wavelength dependence of the scattering from cometary grains; spectral slope provides a complementary perspective on dust properties (Jewitt and Meech, 1986). Changes in dust color are closely related to cometary activity. Color variations may result from activity on the nucleus surface or within the coma, such as outbursts that expose primordial material from the interior of the nucleus and inject it into the coma (Kolokolova et al., 2003; Zubko et al., 2011, 2014). Collisions with other bodies, such as meteoroids, can also expose deep interior material (Ivanova et al., 2015). Additionally, nucleus rotation alters surface illumination, triggering sublimation from different active regions and ejecting varied material (Voitko et al., 2022). Solar radiation pressure further influences particle dynamics by removing some grains from the coma more quickly or causing sublimation and fragmentation (Li JY et al., 2014; Luk'yanyk et al., 2019). Collectively, these processes demonstrate that variations in cometary activity are reflected in coma color. A clear observational example is comet C/2013 X1 (PANSTARRS), for which Shubina et al. (2024) reported pronounced temporal variations in broadband colors (B–V and V–R) and dust production associated with an outburst, indicating a rapid evolution of dust properties and composition within its coma. This shows that changes in cometary activity can be reflected in the comet's color. Figure 1 indicates, also, a connection between strong activity and the formation of morphological structures and color changes (Voitko et al., 2025).

Zubko et al. (2014) analyzed the photopolarimetric response of comet C/1975 V1 (West) and suggested that the volume ratio of Mg-rich silicates to amorphous carbon particles is approximately 1:3 (weakly absorbing : strongly absorbing). Voitko et al. (2024) proposed that the bluest dust colors may be caused by water ice, Mg-rich silicates, amorphous carbon, or a mixture of these compo-

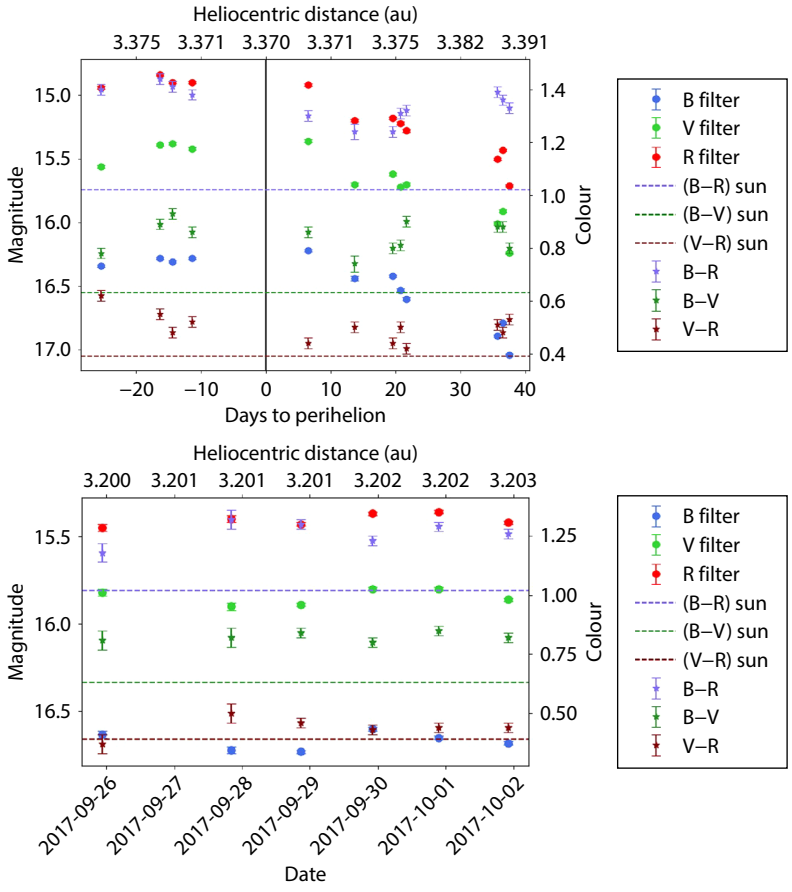

Figure 1. (a) Changes of the apparent magnitude and dust colour of comet C/2020 S4 (PanSTARRS) against days to perihelion. The days to perihelion passage are shown on the lower *x*-axis, where 0 denotes the comet's perihelion passage day. The upper *x*-axis demonstrates the heliocentric distances of the comet at the respective moments. (b) Changes in the apparent magnitude and dust colour of comet C/2017 T2 (PanSTARRS) with time. The upper *x*-axis shows heliocentric distances of the comet at the respective moments. (Voitko et al., 2025).

nents, whereas the reddest colors are likely associated with Mg-Fe silicates and organic materials.

6. Tail Characteristics of LPCs

After the sublimation of solid ices on the cometary nucleus surface, gas is released, carrying dust particles to form the coma. Various structures are often observed in cometary comae, such as jets, fans, and shells. The formation of jets and fan-shaped structures is attributed to nucleus activity, surface heterogeneity, and rotation. Dust shells result from spin-modulated activity, where a single active region periodically becomes exposed to solar radiation due to nucleus rotation, releasing dust into the coma (Whipple, 1978).

Solar radiation pressure pushes dust particles away from the Sun, forming the dust tail, which is usually curved and appears yellowish or whitish. The ion tail, on the other hand, is formed when gas molecules are ionized, primarily by solar ultraviolet photons, and subsequently swept by the solar wind, creating the comet's plasma tail (Biermann, 1951). The velocity at which gas molecules leave the nucleus is comparable to the thermal velocity at the sublimating surface, typically about 1 km/s at 1 au, whereas the comet's orbital motion is closer to the Keplerian velocity, v_K, of tens of km/s. Both velocities are much smaller than the solar wind speed, which ranges from 200 to 2750 km/s as it passes the comet (Hundhausen, 1968); it expands roughly radially outward from the Sun. In interplanetary space, the plasma pressure carried by the solar wind exceeds the magnetic pressure, so the solar magnetic field is effectively frozen into the solar wind. As a result, cometary ions are picked up by the interplanetary magnetic field via the Lorentz force, forming the plasma tail, which generally aligns with the Sun–comet line. Due to these processes, dust and plasma tails are usually spatially separated and appear differently in the sky plane. While the plasma tail is straight and almost radial to the Sun, the dust tail is typically broad and curved in the sky plane due to the combined effects of radiation pressure and orbital motion. The orientations of both tail types should change smoothly with the comet–Sun–observer geometry. Additionally, a very narrow and faint tail is associated with resonant fluorescence of neutral sodium atoms (Cremonese et al., 2002). As shown in Figure 2, three distinct tails were simultaneously observed in Comet C/2020 F3 (NEOWISE): the red component corresponds to the sodium tail, the blue component to the ion tail, and the white component to the dust tail (Afghan et al., 2024).

Short-period comets, having undergone multiple close passages to the Sun, gradually deplete their surface volatiles (e.g., water ice, CO, CO_2), resulting in tails that are typically shorter, fainter, and

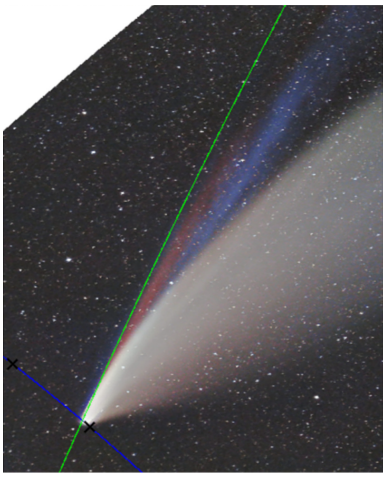

Figure 2. Image of Comet NEOWISE, taken by Mustafa Aydin on July 12, 2020. An atomic sodium tail is visible (with north oriented upward); A bright red tail adjacent to the blue ion tail, a typical feature of atomic sodium tails, is shown in panel (c) of Afghan et al. (2024).

dust-dominated (Reach et al., 2007). In contrast, long-period comets may exhibit activity already at large heliocentric distances, enabling them to develop longer and brighter tails as they enter the inner solar system. Since long-period comets typically preserve a substantial reservoir of unexhausted volatiles, their ion tails are often well-defined, and their intense activity can cause the tail morphology to change rapidly with time (Li J et al., 2023; Zhou YH and Ye Q, 2024). By comparison, short-period comets are relatively deficient in gaseous components, their dust tails are more prominent, and their tail morphologies show less variation, sometimes even displaying a significant degree of predictability (Pozuelos et al., 2014). Overall, most long-period comets display tails, though their prominence does not necessarily correlate with overall brightness, and in some cases the tails appear relatively slender.

There are also peculiar cases. For instance, in the dust tail of long-period comet C/2014 Q1 (PanSTARRS), a distinct gap was observed; Afghan et al. (2023) suggested that this indicates a brief but dramatic reduction in dust emission near perihelion. Comet C/2020 S3 (Erasmus) exhibited a tail-swinging motion at perihelion (0.398 au). Additionally, imaging polarimetry revealed rapid and significant changes in the polarization of its coma over several days, indicating a transition from low P_{max} to high P_{max} classification (Chornaya et al., 2023). This change was attributed to a relative decrease in Mg-rich silicate particles within the coma, reflecting a qualitative change in the dust emission from the comet nucleus. In comets such as C/1858 L1 (Donati), C/1874 H1 (Coggia), C/1881 K1 (Tebbutt), and C/2023 A3 (Tsuchinshan-ATLAS), a dark line structure (DLS) has been observed along the dust tail axis. In particular, studies of the tail morphology of C/2023 A3 (Tsuchinshan-ATLAS) showed that this feature became more pronounced as the comet approached perihelion. Through modeling, as illustrated in Figure 3, Moreno and Jehin (2025) concluded that this phenomenon depends on the relationship between the velocity of tail dust particles and the cosine of the solar zenith angle at the emission point.

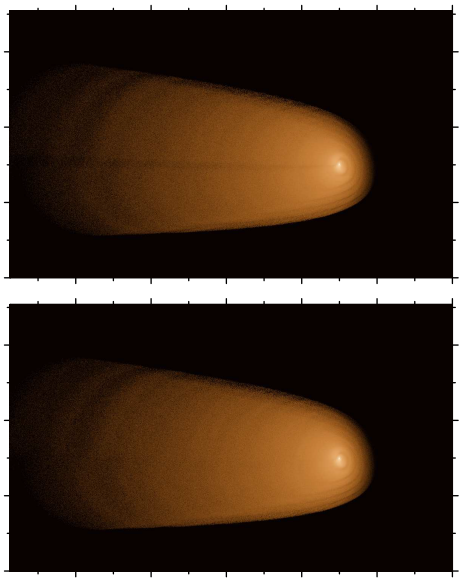

Figure 3. Top panel: Synthetic image to model the dust tail of comet C/1881 K1 (Tebbutt), with $[\lambda_{min}, \lambda_{max}] = [-10°, +85°]$. Bottom panel: Same model as in the top panel but for $[\lambda_{min}, \lambda_{max}] = [-10°, +90°]$, where the DLS vanishes (Moreno and Jehin, 2025).

7. Discussion and Conclusions

The observational window for long-period comets is often very short, and many of them disintegrate shortly after discovery, resulting in a much smaller observational sample size compared with short-period comets. Notably, C/2017 K2 (PANSTARRS), C/2010 U3 (Boattini), C/2014 UN271 (Bernardinelli–Bernstein), and C/2019 E3 (ATLAS) all displayed activity at heliocentric distances beyond 20 au. Compared with other long-period comets, these so-called "ultra-distant comets" exhibited recurrent outbursts and pronounced brightness enhancements as they moved closer to perihelion. However, no clear overall trend can be discerned in the observations of such objects due to their limited sample sizes (Hui MT et al., 2024). In general, long-period comets display stronger activity than short-period comets, but exceptions do exist—for instance, C/2022 E3 (ZTF) exhibited activity at heliocentric distances of 1.7–3.4 au that was more akin to that of short-period comets (Liu B and Liu XD, 2024). This represents an unexpected property among long-period comets, suggesting that there may be deeper connections between short- and long-period comets that remain to be explored. Given the limited number of well-observed distant comets, we summarize characteristics of several representative objects in Table 1, including their perihelion distances, observed activity ranges, proposed activity drivers, and key references. Moreover, cometary outbursts are highly stochastic: some comets undergo outbursts at very large heliocentric distances, while others may erupt multiple times within a single day. Because such events cannot be predicted in advance, observational data on outbursts are often incomplete. Current observational techniques also face limitations in resolving the fine-scale activity of comets at large heliocentric distances, further contributing to the scarcity of data. As a result, many open questions remain regarding the internal structure of cometary nuclei, the triggering mechanisms of gas and dust activity, and the systematic differences between long- and short-period comets.

Table 1. Summary of observations of representative long-period comets exhibiting detectable activity at large heliocentric distances.[a]

Comet	q (au)	Observed activity (au)	Volatiles suggested to contribute to activity	Key reference
C/2010 U3	8.45	≳20	Supervolatile sublimation (CO/CO_2) or crystallization of amorphous water ice	Hui MT et al. (2019)
C/2012 S1	0.01	≳ 5	the annealing of amorphous water ice	Sekanina and Kracht (2015)
C/1995 O1	0.92	≳ 5	CO/CO_2 (≳ 4 au); H_2O (~ 4 au)	Schleicher et al. (2024)
C/1980 E1	3.36	≳ 5	Volatile ice sublimation	A'Hearn et al. (1984)
C/2016 R2	2.60	~ 2.8	CO-dominated, extremely low H_2O	McKay et al. (2019)

[a] The table reports the heliocentric distances at which activity has been observed and lists the volatile species proposed as activity drivers in the literature.

Based on our review of long-period comet (LPC) observations, several key conclusions can be drawn. Long-period comets have a larger semi-major axis and receive less thermal radiation, thus retaining a greater amount of easily sublimable ice. As a result, some LPCs can exhibit significant activity even at large heliocentric distances. Observations have confirmed the presence of H_2O, CO, and CO_2, as well as dust components including Mg-rich silicates and amorphous carbon; perihelion passages may expose more refractory materials, such as olivine-type minerals. Variations in dust composition lead to differences in coma color, while solar radiation produces diverse tail morphologies. Structural features, such as dark stripes and shell-like patterns, provide important constraints on nucleus rotation and the spatial distribution of active regions. Overall, these results highlight how the preserved volatile inventory and nucleus properties shape the observable activity and morphology of LPCs. Despite these insights, our understanding remains limited by the scarcity and heterogeneity of observational data, particularly at large heliocentric distances, pointing to the need for future missions and systematic studies.

Investigating the activity of long-period comets is currently limited by sparse, heterogeneous observations, especially at large heliocentric distances. Future missions, such as Comet Interceptor, as well as proposed in situ and remote-sensing campaigns, will provide more uniform and sensitive measurements of cometary dust and gas activity, composition, and dynamics. These data will help resolve unresolved questions, such as the relative contributions of CO, CO_2, and other volatiles to activity, the physical properties of dust grains, and the processing history of early Solar System and Oort Cloud comets.

By addressing these gaps, studies of long-period comets not only deepen our understanding of their dust and gas dynamics but also offer valuable clues to their origins and evolutionary pathways. Such research lays a critical foundation for probing the Oort Cloud and the formation and evolution of the early Solar System. Moreover, as our understanding of cometary properties advances, long-period comet studies can be expected to contribute to a broader astrophysical context, providing indirect insights into stellar systems beyond our own, since a fraction of Oort Cloud comets may trace their origins to other stars.

Acknowledgments

The research is supported by the Operation, Maintenance and Upgrading Fund for Astronomical Telescopes and Facility Instruments, budgeted from the Ministry of Finance of China (MOF) and administrated by the Chinese Academy of Sciences (CAS), the National Natural Science Foundation of China (grant Nos. 12173093), and science research grants from the China Manned Space Project with No. CMS-CSST-2021-B08.

References

Afghan, Q., Jones, G. H., Price, O., and Coates, A. (2023). Observations of a dust tail gap in comet C/2014 Q1 (PanSTARRS). *Icarus*, *390*, 115286. https://doi.org/10.1016/j.icarus.2022.115286

Afghan, Q., Jones, G. H., Battams, K., Price, O., and Coates, A. J. (2024). Characterization of the dust and sodium tails of comet C/2020 F3 (NEOWISE) from parker solar probe and amateur observations. *Planet. Sci. J.*, *5*(12), 264. https://doi.org/10.3847/PSJ/ad856b

A'Hearn, M. F., Schleicher, D. G., Millis, R. L., Feldman, P. D., and Thompson, D. T. (1984). Comet Bowell 1980b. *Astron. J.*, *89*, 579–591. https://doi.org/10.1086/113552

A'Hearn, M. F., Feaga, L. M., Keller, H. U., Kawakita, H., Hampton, D. L., Kissel, J., Klaasen, K. P., McFadden, L. A., Meech, K. J., … Wellnitz, D. D. (2012). Cometary volatiles and the origin of comets. *Astrophys. J.*, *758*(1), 29. https://doi.org/10.1088/0004-637X/758/1/29

Betzler, A. S., Almeida, R. S., Cerqueira, W. J., Araujo, L. A., Prazeres, C. J. M., Jesus, J. N., Bispo, P. A. S., Andrade, V. B., Freitas, Y. A. S., and Betzler, L. B. S. (2017). An analysis of the BVRI colors of 22 active comets. *Adv. Space Res.*, *60*(3), 612–625. https://doi.org/10.1016/j.asr.2017.04.021

Betzler, A. S., Diepvens, A., and de Sousa, O. F. (2023). The activity of 119 comets. *Mon. Not. R. Astron. Soc.*, *526*(1), 246–262. https://doi.org/10.1093/mnras/stad2696

Biermann, L. (1951). Kometenschweife und solare korpuskularstrahlung. *Zeitschrift Fur Astrophysik*, *29*, 274.

Bockelée-Morvan, D., and Biver, N. (2017). The composition of cometary ices. *Philos. Trans. A Math. Phys. Eng. Sci.*, *375*(2097), 20160252. https://doi.org/10.1098/rsta.2016.0252

Bohren, C. F., and Huffman, D. R. (1998). Absorption and scattering of light by small particles (1st ed.). Wiley. https://doi.org/10.1002/9783527618156

Cambianica, P., Munaretto, G., Cremonese, G., Podio, L., Codella, C., and Boschin, W. (2023). CO_2 as the main parent source of atomic oxygen in comet C/2017 K2 (pan-STARRS). *Astron. Astrophys.*, *674*, L14. https://doi.org/10.1051/0004-6361/202245550

Chornaya, E., Zubko, E., Kochergin, A., Zheltobryukhov, M., Videen, G., Kornienko, G., and Kim, S. S. (2023). C/2020 S3 (Erasmus): Comet with a presumably transient maximum of linear polarization P_{max}. *Mon. Not. R. Astron. Soc.*, *518*(2), 1617–1628. https://doi.org/10.1093/mnras/stac3201

Cremonese, G., Huebner, W. F., Rauer, H., and Boice, D. C. (2002). Neutral sodium tails in comets. *Adv. Space Res.*, *29*(8), 1187–1197. https://doi.org/10.1016/S0273-1177(02)00136-9

Crovisier, J., Leech, K., Bockelée-Morvan, D., Brooke, T. Y., Hanner, M. S., Altieri, B., Keller, H. U., and Lellouch, E. (1997). The spectrum of comet hale-Bopp (C/1995 O1) observed with the infrared space observatory at 2.9

astronomical units from the sun. *Science*, *275*(5308), 1904–1907. https://doi.org/10.1126/science.275.5308.1904

Crovisier, J., Bockelée-Morvan, D., Colom, P., and Biver, N. (2016). Comets at radio wavelengths. *C. R. Phys.*, *17*(9), 985–994. https://doi.org/10.1016/j.crhy.2016.07.020

Fulle, M. (1989). Evaluation of cometary dust parameters from numerical simulations: Comparison with an analytical approach and the role of anisotropic emissions. *Astron. Astrophys.*, *217*, 283–297.

Garcia, R. S., Fernández-Lajús, E., Di Sisto, R. P., and Gil-Hutton, R. A. (2024). Photometric and numerical study of comet C/2021 A1 (Leonard) near its estimated disruption date. *Icarus*, *420*, 116206. https://doi.org/10.1016/j.icarus.2024.116206

Geheimenrath, H., and Bessel, R. (1836). Beobachtungen über die physische Beschaffenheit des *Halley*'schen kometen und dadurch veranlasste bemerkungen. *Astron. Nachr.*, *13*(13-15), 185–232. https://doi.org/10.1002/asna.18360131302

Gehrz, R. D., Johnson, C. H., Magnuson, S. D., Ney, E. P., and Hayward, T. L. (1995). Infrared observations of an outburst of small dust grains from the nucleus of comet P/Halley 1986 III at perihelion. *Icarus*, *113*(1), 129–133. https://doi.org/10.1006/icar.1995.1011

Gronkowski, P., and Smela, J. (1998). The cometary outbursts at large heliocentric distances. *Astron. Astrophys.*, *338*(2), 761–766.

Gronoff, G., Maggiolo, R., Cessateur, G., Moore, W. B., Airapetian, V., De Keyser, J., Dhooghe, F., Gibbons, A., Gunell, H., … Hosseini, S. (2020). The effect of cosmic rays on cometary nuclei. I. Dose deposition. *Astrophys. J.*, *890*(1), 89. https://doi.org/10.3847/1538-4357/ab67b9

Harrington Pinto, O., Womack, M., Fernandez, Y., and Bauer, J. (2022). A survey of CO, CO_2, and H_2O in comets and centaurs. *Planet. Sci. J.*, *3*(11), 247. https://doi.org/10.3847/PSJ/ac960d

Hartogh, P., Lis, D. C., Bockelée-Morvan, D., de Val-Borro, M., Biver, N., Küppers, M., Emprechtinger, M., Bergin, E. A., Crovisier, J., … Blake, G. A. (2011). Ocean-like water in the Jupiter-family comet 103P/Hartley 2. *Nature, 478*(7368), 218-220. https://doi.org/10.1038/nature10519

Haser, L. (1957). Distribution d'intensité dans la tête d'une comète. *Bull. Soc. R. Sci. Liege*, *43*(1), 740–750. https://doi.org/10.3406/barb.1957.68714

Holt, C. E., Knight, M. M., Kelley, M. S. P., Lister, T., Ye, Q. Z., Snodgrass, C., Opitom, C., Kokotanekova, R., Schwamb, M. E., … Greenstreet, S. (2024). Brightness behavior of distant Oort cloud comets. *Planet. Sci. J.*, *5*(12), 273. https://doi.org/10.3847/PSJ/ad8e38

Horne, K. (1986). An optimal extraction algorithm for CCD spectroscopy. *Publ. Astron. Soc. Pac.*, *98*, 609–617. https://doi.org/10.1086/131801

Houpis, H. L. F., and Mendis, D. A. (1981). Dust emission from comets at large heliocentric distances. *Moon Planets*, *25*(4), 397–412. https://doi.org/10.1007/BF00919075

Hui, M.-T., Jewitt, D., and Clark, D. (2017). Pre-discovery observations and orbit of comet C/2017 K2 (PANSTARRS). *The Astronomical Journal*, *155*(1), 25. https://doi.org/10.3847/1538-3881/aa9be1

Hui, M.-T., Farnocchia, D., and Micheli, M. (2019). C/2010 U3 (Boattini): A bizarre comet active at record heliocentric distance. *Astron. J.*, *157*(4), 162. https://doi.org/10.3847/1538-3881/ab0e09

Hui, M.-T., and Ye, Q.-Z. (2020). Observations of disintegrating long-period comet C/2019 Y4 (ATLAS): A sibling of C/1844 Y1 (great comet). *The Astronomical Journal*, *160*, 91. https://doi.org/10.3847/1538-3881/ab9d81

Hui, M.-T., Weryk, R., Micheli, M., Huang, Z., and Wainscoat, R. (2024). Serendipitous archival observations of a new ultradistant comet C/2019 E3 (ATLAS). *Astron. J.*, *167*(3), 140. https://doi.org/10.3847/1538-3881/ad2500

Hundhausen, A. J. (1968). Direct observations of solar-wind particles. *Space Sci. Rev.*, *8*(5), 690–749. https://doi.org/10.1007/BF00175116

Ivanova, O., Neslušan, L., Krišandová, Z. S., Svoreň, J., Korsun, P., Afanasiev, V., Reshetnyk, V., and Andreev, M. (2015). Observations of comets C/2007 D1 (LINEAR), C/2007 D3 (LINEAR), C/2010 G3 (WISE), C/2010 S1 (LINEAR), and C/2012 K6 (McNaught) at large heliocentric distances. *Icarus*, *258*, 28–36. https://doi.org/10.1016/j.icarus.2015.06.026

Ivanova, O., Luk'yanyk, I., Tomko, D., and Moiseev, A. (2021). Photometry and long-slit spectroscopy of the split comet C/2019 Y4 (ATLAS). *Mon. Not. R. Astron. Soc.*, *507*(4), 5376–5389. https://doi.org/10.1093/mnras/stab2306

Jewitt, D., and Meech, K. J. (1986). Cometary grain scattering versus wavelength, or, 'what color is comet dust'?. *Astrophys. J.*, *310*, 937. https://doi.org/10.1086/164745

Jewitt, D., Hui, M. T., Mutchler, M., Weaver, H., Li, J., and Agarwal, J. (2017). A comet active beyond the crystallization zone. *Astrophys. J. Lett.*, *847*(2), L19. https://doi.org/10.3847/2041-8213/aa88b4

Jewitt, D., Agarwal, J., Hui, M. T., Li, J., Mutchler, M., and Weaver, H. (2019). Distant comet C/2017 K2 and the cohesion bottleneck. *Astron. J.*, *157*(2), 65. https://doi.org/10.3847/1538-3881/aaf38c

Jewitt, D., Luu, J., and Li, J. (2025). Demise of kreutz sungrazing comet C/2024 S1 (ATLAS). *Astron. J.*, *169*(2), 105. https://doi.org/10.3847/1538-3881/ada3c0

Kochergin, A., Zubko, E., Chornaya, E., Zheltobryukhov, M., Videen, G., Kornienko, G., and Kim, S. S. (2023). Microphysics of dust in a distant comet C/2017 K2 (PanSTARRS) retrieved by means of polarimetry. *J. Quant. Spectrosc. Radiat. Transf.*, *297*, 108471. https://doi.org/10.1016/j.jqsrt.2022.108471

Kolokolova, L., Lara, L. M., Schulz, R., Stüwe, J. A., and Tozzi, G. P. (2003). Color of an ensemble of particles with a wide power-law size distribution: Application to observations of Comet Hale-Bopp at 3AU. *J. Quant. Spectrosc. Radiat. Transf., 79-80*, 861-871. https://doi.org/10.1016/S0022-4073(02)00324-2

Kolokolova, L., Hanner, M. S., Levasseur-Regourd, A. C., and Gustafson, B. Å. S. (2004). Physical properties of cometary dust from light scattering and thermal emission. In M. C. Festou, et al. (Eds.), *Comets II* (pp. 577-604). Tucson: University of Arizona Press. https://doi.org/10.2307/j.ctv1v7zdq5.37

Kuiper, G. P. (1951). On the origin of the solar system. *Proc. Natl. Acad. Sci. USA*, *37*(1), 1–14. https://doi.org/10.1073/pnas.37.1.1

Lacerda, P., Guilbert-Lepoutre, A., Kokotanekova, R., Inno, L., Epifani, E. M., and Snodgrass, C. (2025). Secular brightness curves of 272 comets. arXiv:2504.00565. https://doi.org/10.48550/arXiv.2504.00565

Larson, S. M., and Sekanina, Z. (1984). Coma morphology and dust-emission pattern of periodic Comet Halley. I - High-resolution images taken at Mount Wilson in 1910. *Astron. J.*, *89*, 571–578. https://doi.org/10.1086/113551

Lasue, J., Levasseur-Regourd, A. C., Hadamcik, E., and Alcouffe, G. (2009). Cometary dust properties retrieved from polarization observations: Application to C/1995 O1 Hale-Bopp and 1P/Halley. *Icarus*, *199*(1), 129–144. https://doi.org/10.1016/j.icarus.2008.09.008

Li, J., Kim, Y., and Jewitt, D. (2023). The wagging plasma tail of comet C/2020 S3 (Erasmus). *Astron. J.*, *166*(6), 270. https://doi.org/10.3847/1538-3881/ad08af

Li, J. Y., Samarasinha, N. H., Kelley, M. S. P., Farnham, T. L., A'Hearn, M. F., Mutchler, M. J., Lisse, C. M., and Delamere, W. A. (2014). Constraining the dust coma properties of comet C/siding spring (2013 A1) at large heliocentric distances. *Astrophys. J. Lett.*, *797*(1), L8. https://doi.org/10.1088/2041-8205/797/1/L8

Lippi, M., Vander Donckt, M., Faggi, S., Moulane, Y., Mumma, M. J., Villanueva, G. L., and Jehin, E. (2023). The volatile composition of C/2021 A1 (Leonard): Comparison between infrared and UV-optical measurements. *Astron. Astrophys.*, *676*, A105. https://doi.org/10.1051/0004-6361/202346775

Liu, B., and Liu, X. D. (2024). Unraveling the dust activity of naked-eye comet C/2022 E3 (ZTF). *Astron. Astrophys.*, *683*, A51. https://doi.org/10.1051/0004-6361/202348663

Luk'yanyk, I., Zubko, E., Husárik, M., Ivanova, O., Svoreň, J., Kochergin, A., Baransky, A., and Videen, G. (2019). Rapid variations of dust colour in comet 41P/Tuttle-Giacobini-Kresák. *Mon. Not. R. Astron. Soc.*, *485*(3), 4013–4023. https://doi.org/10.1093/mnras/stz669

Luu, J. X. (1993). Cometary activity in distant comets: Chiron. *Publ. Astron. Soc. Pac.*, *105*, 946. https://doi.org/10.1086/133260

Maggiolo, R., Gronoff, G., Cessateur, G., Moore, W. B., Airapetian, V. S., De Keyser, J., Dhooghe, F., Gibbons, A., Gunell, H., … Hosseini, S. (2020). The effect of cosmic rays on cometary nuclei. II. Impact on ice composition and structure. *Astrophys. J.*, *901*(2), 136. https://doi.org/10.3847/1538-4357/

abacc3

McKay, A. J., DiSanti, M. A., Kelley, M. S. P., Knight, M. M., Womack, M., Wierzchos, K., Pinto, O. H., Bonev, B., Villanueva, G. L., … Kawakita, H. (2019). The peculiar volatile composition of CO-dominated comet C/2016 R2 (PanSTARRS). *Astron. J.*, *158*(3), 128. https://doi.org/10.3847/1538-3881/ab32e4

Meech, K. J., and Svoreň, J. (2004). Using cometary activity to trace the physical and chemical evolution of cometary nuclei. In M. C. Festou, et al. (Eds.), *Comets II* (pp. 317–336). Tucson: University of Arizona Press. https://doi.org/10.2307/j.ctv1v7zdq5.26

Meech, K. J., Pittichová, J., Bar-Nun, A., Notesco, G., Laufer, D., Hainaut, O. R., Lowry, S. C., Yeomans, D. K., and Pitts, M. (2009). Activity of comets at large heliocentric distances pre-perihelion. *Icarus*, *201*(2), 719–739. https://doi.org/10.1016/j.icarus.2008.12.045

Meech, K. J., Kleyna, J. T., Hainaut, O., Micheli, M., Bauer, J., Denneau, L., Keane, J. V., Stephens, H., Jedicke, R., … Chambers, K. C. (2017). CO-driven activity in comet C/2017 K2 (PANSTARRS). *Astrophys. J.*, *849*(1), L8. https://doi.org/10.3847/2041-8213/aa921f

Milewski, D. G., Masiero, J. R., Pittichová, J., Kramer, E. A., Mainzer, A. K., and Bauer, J. M. (2024). NEOWISE observations of distant active long-period comets C/2014 B1 (Schwartz), C/2017 K2 (pan-STARRS), and C/2010 U3 (Boattini). *Astron. J.*, *167*(3), 99. https://doi.org/10.3847/1538-3881/ad0cf4

Mishchenko, M. I., Rosenbush, V. K., Kiselev, N. N., Lupishko, D. F., Tishkovcts, V. P., Kaydash, V. G., Belskaya, I. N., Efimov, Y. S., and Shakhovskoy, N. M. (2010). *Polarimetric Remote Sensing of Solar System Objects*. Kyiv: PH "Akademperiodyka". https://doi.org/10.15407/akademperiodyka.134.291

Moreno, F., Pozuelos, F., Aceituno, F., Casanova, V., Sota, A., Castellano, J., and Reina, E. (2012). Comet 22p/kopff: Dust environment and grain ejection anisotropy from visible and infrared observations. *Astrophys. J.*, *752*(2), 136. https://doi.org/10.1088/0004-637X/752/2/136

Moreno, F., Pozuelos, F., Aceituno, F., Casanova, V., Duffard, R., López-Moreno, J. J., Molina, A., Ortiz, J. L., Santos-Sanz, P., … Yanamandra-Fisher, P. (2014). On the dust environment of comet C/2012 S1 (ISON) from 12 AU pre-perihelion to the end of its activity around perihelion. *Astrophys. J.*, *791*(2), 118. https://doi.org/10.1088/0004-637X/791/2/118

Moreno, F. (2022). Monte Carlo models of comet dust tails observed from the ground. *Universe*, *8*(7), 366. https://doi.org/10.3390/universe8070366

Moreno, F., and Jehin, E. (2025). Dust shells and dark linear structures on dust tails of historical and recent long-period comets. arXiv:2503.10121. https://doi.org/10.48550/arXiv.2503.10121

Mumma, M. J., and Charnley, S. B. (2011). The chemical composition of comets—Emerging taxonomies and natal heritage. *Annu. Rev. Astron. Astrophys.*, *49*(1), 471–524. https://doi.org/10.1146/annurev-astro-081309-130811

Musiolik, G., Teiser, J., Jankowski, T., and Wurm, G. (2016). Collisions of CO_2 ice grains in planet formation. *Astrophys. J.*, *818*(1), 16. https://doi.org/10.3847/0004-637X/818/1/16

Oort, J. H. (1950). The structure of the cloud of comets surrounding the solar system and a hypothesis concerning its origin. *Bull. Astron. Inst. Netherlands*, *11*, 91–110.

Pozuelos, F. J., Moreno, F., Aceituno, F., Casanova, V., Sota, A., López-Moreno, J. J., Castellano, J., Reina, E., Climent, A., … Pastor, S. (2014). Dust environment and dynamical history of a sample of short-period comets. II. 81P/wild 2 and 103P/Hartley 2. *Astron. Astrophys.*, *571*, A64. https://doi.org/10.1051/0004-6361/201424331

Prialnik, D. (1992). Crystallization, sublimation, and gas release in the interior of a porous comet nucleus. *Astrophys. J.*, *388*, 196. https://doi.org/10.1086/171143

Prialnik, D., Benkhoff, J., and Podolak, M. (2004). Modeling the structure and activity of comet nuclei. In M. C. Festou, et al. (Eds.), *Comets II* (pp. 359-388). Tucson: University of Arizona Press. https://doi.org/10.2307/j.ctv1v7zdq5.28

Prialnik, D., and Jewitt, D. (2024). Amorphous ice in comets: Evidence and consequences. In K. J. Meech et al. (Eds.), *Comets III* (pp. 823-844) Tucson: University of Arizona Press. https://doi.org/10.2458/azu_uapress_9780816553631-ch025

Qi, C. H., Öberg, K. I., Wilner, D. J., D'Alessio, P., Bergin, E., Andrews, S. M., Blake, G. A., Hogerheijde, M. R., and van Dishoeck, E. F. (2013). Imaging of the CO snow line in a solar nebula analog. *Science*, *341*(6146), 630–632. https://doi.org/10.1126/science.1239560

Reach, W. T., Kelley, M. S., and Sykes, M. V. (2007). A survey of debris trails from short-period comets. *Icarus*, *191*(1), 298–322. https://doi.org/10.1016/j.icarus.2007.03.031

Rettig, T. W., Tegler, S. C., Pasto, D. J., and Mumma, M. J. (1992). Comet outbursts and polymers of HCN. *Astrophys. J.*, *398*, 293. https://doi.org/10.1086/171857

Schleicher, D. G., Birch, P. V., Farnham, T. L., and Bair, A. N. (2024). The extreme activity in Comet Hale–Bopp (C/1995 O1): Investigations of extensive narrowband photoelectric photometry. *Planet. Sci. J.*, *5*(12), 281. https://doi.org/10.3847/PSJ/ad86b9

Schulz, R., Arpigny, C., Manfroid, J., Stüwe, J. A., Tozzi, G. P., Rembor, K., Cremonese, G., and Peschke, S. (1998). Spectral evolution of Rosetta target comet 46P/Wirtanen. *Astron. Astrophys.*, *335*, L46–L49. https://doi.org/10.1007/978-94-011-4211-3_29

Sekanina, Z., and Kracht, R. (2015). Disintegration of comet C/2012 S1 (ISON) shortly before perihelion: Evidence from independent data sets. arXiv:1404.5968. https://doi.org/10.48550/arXiv.1404.5968

Shubina, O., Zubko, E., Kleshchonok, V., Ivanova, O. V., Husárik, M., and Videen, G. (2024). Dust properties and their variations in comet C/2013 X1 (PANSTARRS). *Astron. Astrophys.*, *687*, A297. https://doi.org/10.1051/0004-6361/202449145

Sonka, A. B., Birlan, M., and Nedelcu, D. A. (2020). Monitoring the fragmentation of C/2019 Y4 (ATLAS). *Romanian Astron. J.*, *30*(2), 153–163.

Taylor, M. G. G. T., Altobelli, N., Buratti, B. J., and Choukroun, M. (2017). The Rosetta mission orbiter science overview: The comet phase. *Philos. Trans. A: Math. Phys. Eng. Sci.*, *375*(2097), 20160262. https://doi.org/10.1098/rsta.2016.0262

Voitko, A., Zubko, E., Ivanova, O., Luk'yanyk, I., Kochergin, A., Husárik, M., and Videen, G. (2022). Color variations of comet 29P/Schwassmann-Wachmann 1 in 2018. *Icarus*, *388*, 115236. https://doi.org/10.1016/j.icarus.2022.115236

Voitko, A., Zubko, E., Ivanova, O., Husárik, M., and Videen, G. (2024). Dust color variations of comet C/2016 M1 (PanSTARRS). *Icarus*, *411*, 115967. https://doi.org/10.1016/j.icarus.2024.115967

Voitko, A., Kleshchonok, V., Shubina, O., Ivanova, O., and Husárik, M. (2025). Photometric study of eight distant comets. *Mon. Not. R. Astron. Soc.*, *538*(3), 1609–1627. https://doi.org/10.1093/mnras/staf400

Weaver, H. A. (1989). The volatile composition of comets. *Highlights Astron.*, *8*, 387–393. https://doi.org/10.1017/S1539299600008030

Whipple, F. L. (1950). A comet model. I. The acceleration of comet Encke. *Astrophys. J.*, *111*, 375–394. https://doi.org/10.1086/145272

Whipple, F. L. (1978). Rotation period of comet Donati. *Nature*, *273*(5658), 134–135. https://doi.org/10.1038/273134a0

Yang, B., Jewitt, D., Zhao, Y. H., Jiang, X. J., Ye, Q. Z., and Chen, Y. T. (2021). Discovery of carbon monoxide in distant comet C/2017 K2 (PANSTARRS). *Astrophys. J. Lett.*, *914*(1), L17. https://doi.org/10.3847/2041-8213/ac03b7

Ye, Q. Z., Jewitt, D., Hui, M. T., Zhang, Q. C., Agarwal, J., Kelley, M. S. P., Kim, Y., Li, J., … Weaver, H. A. (2021). Disintegration of long-period comet C/2019 Y4 (ATLAS). I. Hubble space telescope observations. *Astron. J.*, *162*(2), 70. https://doi.org/10.3847/1538-3881/abfec3

Zhang, Q. C., Kolokolova, L., Ye, Q. Z., and Vissapragada, S. (2022). Dust evolution in the coma of distant, inbound comet C/2017 K2 (PANSTARRS). *Planet. Sci. J.*, *3*(6), 135. https://doi.org/10.3847/PSJ/ac6d58

Zhao, R. N., Li, A. G., Yang, B., Wang, L., Wang, H. J., Liu, Y. J., and Liu, J. F. (2024). Dust and volatiles in the disintegrating comet C/2019 Y4 (ATLAS). *Astrophys. J.*, *963*(2), 90. https://doi.org/10.3847/1538-4357/ad1ab7

Zheltobryukhov, M., Zubko, E., Chornaya, E., Kochergin, A., Hines, D. C., and Videen, G. (2023). On the extremely low polarization in comet C/2023 P1 (Nishimura). *Mon. Not. R. Astron. Soc.: Lett.*, *528*(1), L117–L121. https://doi.org/10.1093/mnrasl/slad181

Zhou, Y. H., and Ye, Q. (2024). Tail morphology of near-sun comet C/2020 F3 (NEOWISE). *Res. Notes AAS*, *8*(7), 189. https://doi.org/10.3847/2515-5172/ad6860

Zubko, E., Furusho, R., Kawabata, K., Yamamoto, T., Muinonen, K., and Videen, G. (2011). Interpretation of photo-polarimetric observations of comet 17P/Holmes. *J. Quant. Spectrosc. Radiat. Transf.*, *112*, 1848–1863. https://doi.org/10.1016/j.jqsrt.2011.01.020

Zubko, E., Muinonen, K., Videen, G., and Kiselev, N. N. (2014). Dust in comet C/1975 V1 (west). *Mon. Not. R. Astron. Soc.*, *440*(4), 2928–2943. https://doi.org/10.1093/mnras/stu480

Zubko, E., Chornaya, E., Zheltobryukhov, M., Matkin, A., Ivanova, O. V., Bodewits, D., Kochergin, A., Kornienko, G., Luk'yanyk, I., … Videen, G. (2020a). Extremely low linear polarization of comet C/2018 V1 (Machholz-Fujikawa-Iwamoto). *Icarus*, *336*, 113453. https://doi.org/10.1016/j.icarus.2019.113453

Zubko, E., Zheltobryukhov, M., Chornaya, E., Kochergin, A., Videen, G., Kornienko, G., and Kim, S. S. (2020b). Polarization of disintegrating comet C/2019 Y4 (ATLAS). *Mon. Not. R. Astron. Soc.*, *497*(2), 1536–1542. https://doi.org/10.1093/mnras/staa1725